Interactions between Domains of Apo Calmodulin Alter Calcium Binding and Stability†

Brenda R. Sorensen and Madeline A. Shea*

Department of Biochemistry, University of Iowa College of Medicine, Iowa City, Iowa 52242-1109

Received July 28, 1997; Revised Manuscript Received January 21, 1998

ABSTRACT: Calmodulin (CaM) is an essential protein that exerts exquisite spatial and temporal control over diverse eukaryotic processes. Although the two half-molecule domains of CaM each have two EF-hands and bind two calcium ions cooperatively, they have distinct roles in activation of some targets. Interdomain interactions may mediate coordination of their actions. Proteolytic footprinting titrations of CaM [Pedigo and Shea (1995) *Biochemistry* 34, 1179−1196; Shea, Verhoeven, and Pedigo (1996) *Biochemistry 35*, 2943−2957] showed that calcium binding to the high-affinity sites (III and IV in the C-domain) alters the conformation of helix B in the N-domain despite sites I and II being vacant. This may arise from calcium-induced disruption of interactions between the apo domains. In this study, comparing the cloned domains (residues 1−75, 76−148) to whole CaM, the proteolytic susceptibility of helix B in the apo isolated N-domain was higher than in apo CaM. The isolated N-domain was monotonically protected by calcium binding and had a higher calcium affinity than when part of whole CaM. The change in affinity was small (1−1.5 kcal/mol) but acted to separate the domain saturation curves of whole CaM. Unfolding enthalpies and melting temperatures of the apo isolated domains did not correspond to the two transitions resolved for apo CaM. In summary, the interactions between domains of apo CaM protected the N-domain from proteolysis and raised its T_m by 10 °C, demonstrating that CaM is not the sum of its parts.

A fundamental challenge in biology is to understand quantitatively how physicochemical properties of regulatory proteins control complex cellular phenomena at the molecular level. Calmodulin (CaM),[1] having only 148 amino acids, is the primary intracellular calcium sensor in eukaryotic cells and is a member of the EF-hand family of proteins (*1*, *2*) (see Figure 1A). Calcium binds to CaM cooperatively, opening hydrophobic clefts in both domains that activate it to regulate myriad tissue-specific cellular processes including metabolic and developmental pathways as well as motility and neurotransmission (see *3*). Understanding the molecular mechanism of these processes requires determination of the number and properties of conformational states populated by calmodulin, the intrinsic free energies of calcium binding to each of the four sites, and the degree of intradomain and interdomain cooperativity.

Calmodulin has a repetitive sequence configured in an α−β−α′−β′ pattern of EF-hand (helix−loop−helix) motifs. The N-domain (defined as residues 1−75) and C-domain (defined as residues 76−148) appear similar and independent on the basis of comparison by sequence and available structures. Each consists of two EF-hands linked by a short region of antiparallel β sheet as seen in structures of calcium-saturated CaM determined both in the absence (see Figure 1B) and in the presence of target peptides or drugs (see *4* for review). The calcium binding sites are comprised of 12 highly conserved residues (see Figure 1A), 5 of which are directly involved in the pentagonal bipyramidal chelation of calcium ion [labeled X, Y, Z, −Y, −X, and −Z (cf. *5*)]. The helices are designated by letters beginning at the N-terminus (e.g., helices A and B flank site I). Intramolecular interactions between paired sites in each domain of CaM mediate positive cooperativity of calcium binding (see *5*−*7*).

The domains have distinct roles in activation of some target proteins (*8*−*10*). Thus, both the number and position of calcium ions bound to CaM may regulate its interactions with targets (*11*−*13*). In all crystallographic structures of calcium-saturated CaM (in the absence of a target peptide or drug), the domains form two ends of a dumbbell shape which arises because the axes of the D-helix (in the N-domain) and the E-helix (in the C-domain) are aligned to form a single seven-turn α-helix (see Figure 1B). However, the structure of the linker region between domains appears to be variable and highly dependent on solution conditions (*14*). NMR studies of calcium-saturated CaM indicated this

† These studies were supported by grants to M.A.S. from the American Heart Association (910148980) and the National Science Foundation Presidential Young Investigator Award (NSF DMB 9057157) and to the University of Iowa (NIH BRS Shared Instrumentation Grant S10 RR10409).

* Corresponding author. Telephone: (319) 335-7885. E-mail: madeline-shea@uiowa.edu.

[1] Abbreviations: BAPTA, 1,2-bis(*o*-aminophenoxy)ethane-*N*,*N*,*N*′,*N*′-tetraacetic acid; CaM, calmodulin (1−148); CD, circular dichroism; *dif*BAPTA, 4,4′-difluoro-BAPTA; EGTA, ethylene glycol bis(β-aminoethyl ether)-*N*,*N*,*N*′,*N*′-tetraacetic acid; EndoGluC, endoproteinase GluC; FFRCK, Phe-Phe-Arg-chloromethyl ketone; HEPES, *N*-(2-hydroxyethyl)piperazine-*N*′-2-ethanesulfonic acid; HPLC, high-performance liquid chromatography; NTA, nitrilotriacetic acid; SDS−PAGE, sodium dodecyl sulfate−polyacrylamide gel electrophoresis; TFA, trifluoroacetic acid.

S0006-2960(97)01820-5 CCC: $15.00
Published on Web 02/27/1998

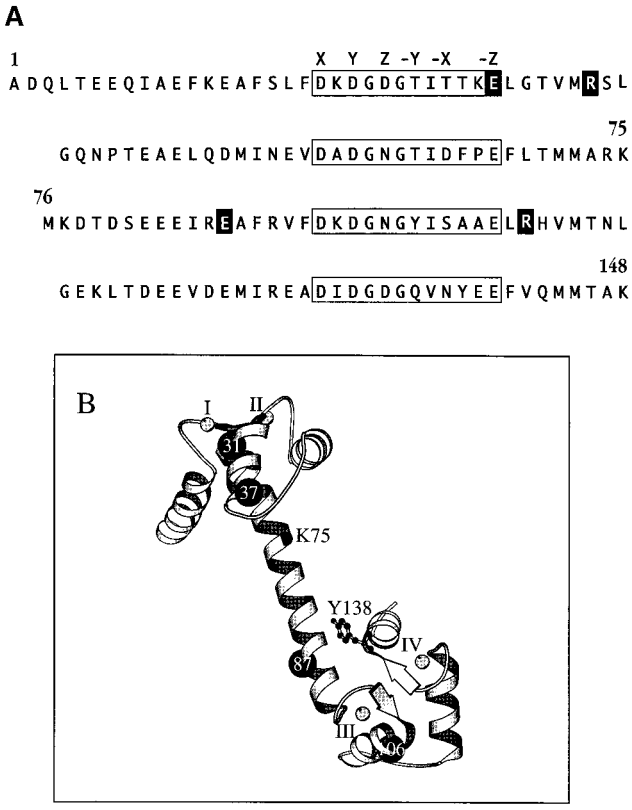

FIGURE 1: (A) Amino acid sequence of rat CaM aligned as four homologous segments. The N-domain (residues 1−75) contains calcium-binding sites I and II, and the C-domain (residues 76−148) contains calcium-binding sites III and IV. The 12 residues comprising each site are boxed, and those involved in chelating calcium ion are in positions X, Y, Z, −Y, and −Z. Sites of proteolysis by EndoGluC (E31, E87) and thrombin (R37, R106) are highlighted. (B) Ribbon drawing (*67*) of the α-carbon backbone of a crystallographic structure of Ca^{2+}_4-CaM (*68*) in which residues 5−147 were resolved. Coordinates were taken from the Brookhaven Protein Data Bank file 3cln.pdb (*69*, *70*). The calcium-binding sites are numbered with Roman numerals. Lysine 75 is highlighted to illustrate where the protein was divided in the bacterial overexpression of the isolated N- and C-domains. Glutamates 31 and 87 are EndoGluC cleavage sites, and arginines 37 and 106 are thrombin cleavage sites monitored in the quantitative proteolytic footprinting studies presented here. The intrinsic tyrosine fluorescence of Y138 changes upon calcium binding.

extended D−E helix was disrupted by four nonhelical residues from D78 to S81 (*15*). Other studies have shown that the helix can be "hinged" or serve as a flexible tether in the absence of targets (*16*−*21*).

Many studies have concluded the two domains in both the apo and calcium-saturated forms of CaM are structurally autonomous (cf. *22*). However, there is qualitative and quantitative evidence that the domains interact over the course of a calcium titration (*23*−*32*). Interpretation of some of these studies is complicated by the evidence that the affinities of the domains are not completely separated in wild-type CaM (i.e., that sites I and II begin to saturate before sites III and IV are fully saturated).

Quantitative proteolytic footprinting studies of wild-type CaM titrations (*23*, *24*) provided direct evidence that calcium binding at the high-affinity sites (III and IV) in the C-domain alters the susceptibility of the backbone in the apo N-domain. Constraints on the apo N-domain are modified such that it becomes susceptible to proteolysis in helix B (at E31, R37, and S38) although sites I and II are still vacant. Subsequent binding of calcium to those sites then causes the N-domain to adopt a third structure (i.e., not susceptible to proteolysis and saturated with calcium). The pattern alternates as indicated by the shaded "cut" blocks in the schematic diagram below. Thus, the apo N-domain and C-domain are not equivalent. There are two forms of the apo N-domain resulting in a doubly saturated intermediate that is not the average of the end states.

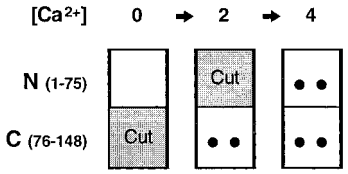

The interplay between local binding interactions and global conformational change form the basis of the switching processes triggered by calcium binding. The difference in susceptibility between the N-domain and the C-domain in the apo state of CaM highlights their nonequivalent structural properties. We wished to determine whether the structural interactions of domains (e.g., the effect of sites III and IV on helix B) have significant energetic consequences on calcium binding. Thus, we compared the properties of whole calmodulin (CaM) to those of isolated (overexpressed) half-molecule domains (see Figure 1 for boundaries). This approach has been used successfully to explore several aspects of calmodulin function by examining fragments generated proteolytically (*31*−*36*).

The intrinsic calcium binding properties of both domains were estimated from analysis of titrations monitored by fluorescence intensity and quantitative proteolytic footprinting. Thermal unfolding studies monitored by CD were used to explore whether interdomain interactions occur in the absence of calcium. Contrary to studies reporting that whole CaM is simply a sum of its parts, the N-domain had a higher affinity for calcium when it was an isolated peptide while the isolated C-domain was almost unchanged in affinity. The apo isolated domains had equivalent melting temperatures (∼50 °C) that separated by almost 12 °C in whole CaM; the total enthalpy of unfolding differed by 6 kcal/mol. Thus, interdomain interactions appeared to widen the difference between properties of the isolated domains which may be physiologically significant to those proteins that interact differentially with one domain or the other. A preliminary report of this work appeared previously (*37*).

EXPERIMENTAL PROCEDURES

Materials. Fluorimetric probes (BAPTA and 4,4′-difluoro-BAPTA) were purchased from Molecular Probes (Eugene, OR). Thrombin (EC 3.4.21.5; catalog no. 605190) and its inhibitor (FFRCK; catalog no. 520218) were purchased from Calbiochem (San Diego, CA), and EndoGluC (EC 3.4.21.19, EndoGluC) was purchased from Promega (Madison, WI). Solvents for HPLC and other routine laboratory chemicals were of the highest grade commercially available.

Cloning and Purification. Recombinant rat calmodulin (CaM) was overexpressed in *E. coli* using the T7-7 vector (*38*, *39*) in Lys-S cells (U. S. Biochemicals, Cleveland, OH)

as described previously (*23*). The isolated N-domain (residues 1−75 of CaM) and C-domain (residues 76−148) were created using standard cloning techniques (*40*). The numbering scheme refers to the corresponding residue of whole CaM (i.e., the first residue of the isolated C-domain is referred to as residue 76). Recombinant proteins were purified to approximately 99% purity as judged by silver staining of overloaded reducing SDS−PAGE and by small-zone gel permeation chromatography and stored at −20 °C.

Titrations Monitored by Fluorescence. Fluorescence studies were carried out at 22 °C using an SLM 4800 on protein at 3 μM in 50 mM HEPES, 100 mM KCl, 0.5 mM EGTA, 0.5 mM NTA, 4 μM *dif*BAPTA, pH 7.40. Free calcium was determined by the degree of saturation of *dif*BAPTA as described previously (*23*, *41*). The titrations were repeated at least 3 times. Rat CaM contains no tryptophan and only two tyrosine residues, both located in the C-domain (Y99 and Y138). Only tyrosine 138 (see Figure 1B; in site IV) shows a calcium-dependent change in fluorescence, and almost all of the change in signal is attributable to calcium binding to sites III and IV (see discussion in *23*). Therefore, only CaM and the C-domain could be studied this way.

Proteolytic Footprinting Titrations. Quantitative proteolytic footprinting of discontinuous equilibrium titrations was analogous to previous studies (*23*, *24*); extensive controls on suitable reaction conditions are described therein. Aliquots of CaM and the isolated N- and C-domains were dialyzed simultaneously and extensively in a series of buffers containing 50 mM HEPES, 91.4 ± 0.7 mM KCl, 5 mM NTA, and 0.05 mM EGTA; pH 7.40 ± 0.01 at 22.0 ± 0.2 °C with added $CaCl_2$. The net free calcium level was determined experimentally using a fluorimetric indicator (with a K_d of 1.52×10^{-6} M^{-1} for *dif*BAPTA and 1.26×10^{-7} M^{-1} for BAPTA) or calcium-selective electrode (F2110Ca; Radiometer); pCa ($-\log[Ca^{2+}]_{free}$) values ranged from 9.48 (apo) to 3.67 (saturated). Protein dialysates were diluted in the corresponding pCa buffer to 0.2 mg/mL (12 μM CaM, 24 μM N- and C-domains) and subjected to limited proteolysis separately. Identification of cleavage products for whole CaM had been performed previously (*23*, *24*). The cleavage products of isolated domains were identified with mass spectroscopy (MALDI-TOF from PerSeptive Biosystems, Inc.). Calculations based on assuming cleavage positions of E31, R37, E87, and R106 (*23*, *24*) yielded values of percent accuracy ([theoretical mass]/[experimental mass]) of fragment identification of >99%.

Thrombin Footprinting. Conditions for limited proteolysis of whole CaM by thrombin had been established (*24*). For the isolated N-domain, 0.01 unit/μL thrombin was used for 0.2 mg/mL N-domain (the same molar ratio of protease to protein that was used for whole CaM). For the isolated C-domain, 0.05 unit/μL thrombin was used for 0.2 mg/mL C-domain (5 times the molar ratio of protein to protease that was used for whole CaM) because the intrinsic susceptibility of the R106−H107 bond in the isolated C-domain in the absence of calcium was lower than was observed for whole CaM under identical conditions. Samples were incubated for 60 min at 22.0 °C, and FFRCK was added to inhibit proteolysis. Products of limited proteolysis were separated and quantified using rpHPLC.

EndoGluC Footprinting. Conditions for limited proteolysis of whole CaM by EndoGluC had been established (*23*). To minimize secondary cleavage by EndoGluC, the mass ratio of protease to CaM was low (1:100). To maintain the corresponding molar ratio, twice the mass ratio was used for proteolytic footprinting of the isolated N- and C-domains (1:50). Reactions were quenched by injection onto a rpHPLC column.

Analysis of ΔG *of Calcium Binding*. The Gibbs free energies of calcium binding were obtained from fits of the titration data to an Adair function (eq 1; *23*, *24*) which allows the pair of sites within a domain (i.e., sites I and II in the N-domain or sites III and IV in the C-domain) to be heterogeneous (i.e., non-identical) and cooperative.

$$\overline{Y_{II}} = \frac{K_1[X]_1 + 2K_2[X]^2}{2(1 + K_1[X]^1 + K_2[X]^2)} \quad (1)$$

The macroscopic equilibrium constant K_1 ($\Delta G_1 = -RT \ln K_1$) in eq 1 represents the sum of two intrinsic constants (k_1 and k_2) that are not necessarily equal. The macroscopic constant K_2 ($\Delta G_2 = -RT \ln K_2$) represents the equilibrium constant for binding ligand to both sites (the product of k_1, k_2, and k_{12}); it accounts for any positive or negative cooperativity. Data for each peptide were normalized first to the highest and lowest experimentally determined values. To account for finite variations in the asymptotes of the susceptibility profiles for different peptides, the function [$f(X)$] used for nonlinear least-squares analysis of the fractional abundance of each peptide was given by

$$f(X) = Y_{[x]_{low}} + \overline{Y}_t \cdot span \quad (2)$$

where $\bar{Y}_t$ refers to the average fractional saturation as described by eq 1 and $Y_{[x]_{low}}$ corresponds to the value of the susceptibility at the lowest calcium concentration of the titration being fit (*24*). Note that *span* is negative for a monotonically decreasing signal. Values for all parameters were fit simultaneously; for biphasic susceptibility profiles, the *span* was fixed at 1.1 or −1.1. Data for complementary primary cleavage products were fit separately and as combined sets (Tables 1 and 2). Criteria reported by *nonlin* (*42*) used for evaluating goodness-of-fit included (a) the value of the square root of variance, (b) the values of asymmetric 65% confidence intervals, (c) the systematic trends in the distribution of residuals, (d) the magnitude of the span of residuals, and (e) the absolute value of elements of the correlation matrix. An estimate of the free energy of cooperativity was made with eq 3.

$$\Delta G_c = \Delta G_2 - 2\Delta G_1 - RT \ln 4 \quad (3)$$

The value of ΔG_c cannot indicate positive cooperativity if there is none, but the precise numerical value may be in error if the fundamental assumption about equivalency of sites ($k_1 = k_2$) is faulty. This estimate is used as a diagnostic indicating the nature of intradomain cooperativity, but there is little significance to small numerical differences between resolved values (see *43* for discussion). In the analysis of calcium binding titrations, the resolved parameters that gave the best fit indicated positive cooperativity (ΔG_c) as had been found in previous studies. A model forcing the sites to be

equal and independent ($\Delta G_c = 0$) was found unacceptable on the basis of sinusoidal residuals (cf. Figure 3 of *23* and Figure 6 of *24*).

Gel Permeation Chromatography. Gel permeation chromatography studies of the isolated N- and C-domains were performed as described previously (*44*). The isolated domains were studied at pCa 8.86 ± 0.18 (apo) and pCa 2.84 ± 0.01 (saturated).

Analytical Ultracentrifugation. To test for self-association at 22 °C, sedimentation equilibrium studies were conducted using a Beckman XL-I analytical ultracentrifuge with six-channel equilibrium centerpieces (*40*). Purified proteins were dialyzed extensively against 2 L of buffer A (50 mM HEPES, 100 mM KCl, 8 mM $CaCl_2$, pH 7.40) or buffer B (50 mM HEPES, 100 mM KCl, 8 mM EGTA, pH 7.40). Concentrations were 19.3 mg/mL (apo CaM), 29.1 mg/mL (apo N-domain), 14.8 mg/mL (apo C-domain), 22.9 mg/mL (Ca^{2+}_4-CaM), 33.5 mg/mL (Ca^{2+}_2-N-domain), and 18.0 mg/mL (Ca^{2+}_2-C-domain). Using the dialysis buffers, proteins were diluted to 0.5, 5, and 15 mg/mL. A mixture of the isolated N- and C-domains was prepared by diluting the N- and C-domain dialysates to either 0.5, 3, or 7 mg/mL of each protein.

Absorbances of CaM, the isolated C-domain, and the mixture of the isolated N- and C-domain samples at 0.5 mg/mL concentrations were taken at 280 nm. The lack of tyrosine and tryptophan residues in the isolated N-domain required the use of a shorter wavelength (240 nm) for detection of this domain. The same samples at higher concentrations (5 and 15 mg/mL or 3 and 7 mg/mL for the mixture of the isolated domains) were analyzed using interference optics. Individual proteins were centrifuged at 15 000, 20 000, and 25 000 rpm; the mixture of the isolated N- and C-domains was centrifuged at 18 000, 23 000, and 28 000 rpm. Data were fit to models for monomer, oligomers, and nonideal species using HID, a nonlinear least-squares analysis program written for the IBM-PC by Jeff Lary (University of Connecticut).

Thermal Unfolding Monitored Spectrally. Thermal unfolding was conducted on an AVIV 62DS CD spectrometer equipped with a thermoelectric temperature controller and an immersible thermocouple, accurate to ±0.4 °C. Proteins were diluted to 15 μM in a total volume of 3 mL of 2 mM HEPES, 100 mM KCl, pH 7.40, and depleted of calcium with the addition of buffered EGTA (>2-fold excess over calcium sites). Samples were denatured at a rate of 1 °C/min. Ellipticity at 222 nm was averaged for 20 s every 30 s and stored with experimental measurements of temperature. Analysis of curves obtained from re-unfolding the same sample or increasing the rate of unfolding to 2 °C/min resulted in equivalent $\Delta H°_{VH}$ and T_m values. The maximum temperature reached in these unfolding studies was 96 °C; however, complete unfolding was observed at 80 °C for all three proteins. The pH of the sample decreased from 7.40 to 7.12 with heating to 92 °C. Samples were rapidly cooled to 0 °C; the percent renaturation for CaM was 95.6 ± 0.5%, N-domain was 97.4 ± 0.7%, and C-domain was 94.3 ± 1.7% (all values calculated on the basis of at least three trials).

Analysis of $\Delta H°_{VH}$ and T_m. The data from thermal denaturation of CaM and the isolated N-domain and C-domain in the absence of calcium were fit to two models of unfolding using *nonlin* (*42*). A two-state model (eq 4) describes unfolding as a single transition between a native (N) and an unfolded (U) state.

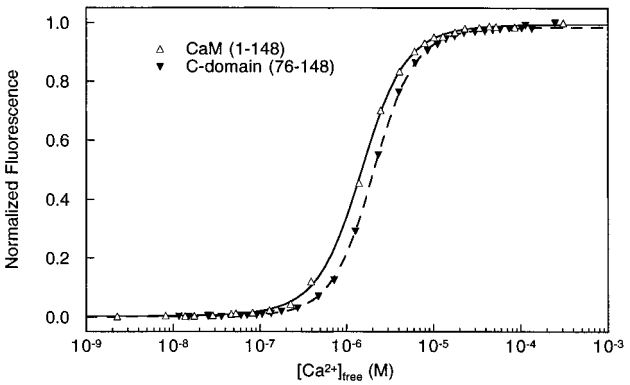

FIGURE 2: Calcium titration of calmodulin (△) and the isolated C-domain (▼) monitored by fluorescence. Curves simulated with values from Table 2.

$$Y_{obs} = f_N(y_{N+m_N}T) + f_U(y_{U+m_U}T) \quad (4)$$

A three-state model (eq 5) describes the unfolding of protein in two transitions: native (N) denatures to an intermediate (I) which then denatures to an unfolded (U) state.

$$Y_{obs} = f_N(y_{N+m_N}T) + f_I(y_{I+m_I}T) + f_U(y_{U+m_U}T) \quad (5)$$

The experimental observable (molar ellipticity in deg·cm^2/dmol) was fit to these equations (*45*), where f is the fraction of the total population of protein in solution that occupies the native (f_N), intermediate (f_I), and unfolded (f_U) forms, y is the intercept, and m_i terms are the slopes of the signals for the native, intermediate, and unfolded forms of calmodulin. A plateau for an intermediate in the unfolding transitions was not apparent. Therefore, the slope of the intermediate base line was fixed to have the value of the average of the base lines for the native (m_N) and unfolded (m_U) species. The contribution of each species to the overall observed spectral signal was estimated based on its fractional population (f) determined on the basis of the equilibrium constants for unfolding between each species ($K_i = \exp(-\Delta G_i/RT)$) using a modified Gibbs−Helmholtz equation (eq 6):

$$\Delta G_i = \Delta H_i\left(1 - \frac{T}{T_{m_i}}\right) + \Delta C_{p_i}\left[(T - T_{m_i}) - T\ln\frac{T}{T_{m_i}}\right] \quad (6)$$

where $\Delta H°_i$ is the van't Hoff enthalpy and ΔC_{p_i} is the heat capacity where the subscript i refers to a specific transition (i.e., N−I or I−U transition) (*45*, *46*). In fitting the unfolding data for CaM and the domains to a two-state model (eq 4), all parameters were allowed to vary. However, in fitting the data for CaM to a three-state model (eq 5), ΔC_{p_i} had to be fixed at 0. Criteria for the "goodness-of-fit" were applied as described above for resolution of free energies of calcium binding.

RESULTS

Calcium-Binding Monitored by Fluorescence. Titrations of CaM and the isolated C-domain were monitored by the change in intrinsic tyrosine fluorescence to estimate the energy of calcium binding to sites III and IV as shown in Figure 2. The data were fit to eq 1, and all parameters (ΔG_1,

Table 1: Calcium Binding to Sites III and IV of CaM Monitored by Fluorescence and Quantitative Proteolytic Footprinting

protein	residue	peptide	ΔG_1[a]	ΔG_2	ΔG_c[b]	$\sqrt{\text{Var}}$
CaM	Y138		-6.94 ± 0.11	-15.61 ± 0.02	-2.55 ± 0.22	0.005
C-domain	Y138		-6.83 ± 0.11	-15.36 ± 0.02	-2.52 ± 0.21	0.005
CaM	E87	both[c]	-7.14 ± 0.70	-15.66 ± 0.17	$-2.20 + 1.00_{-\infty}$	0.073
		1−87	-6.88 ± 1.46	-15.55 ± 0.26	$-2.61 + 1.88_{-\infty}$	0.080
		88−148	-7.29 ± 1.14	-15.79 ± 0.16	-2.02 ± 2.29	0.043
C-domain	E87	both	-6.91 ± 0.88	-15.73 ± 0.08	-2.74 ± 1.75	0.033
		76−87	-6.91 ± 1.54	-15.73 ± 0.26	$-2.72 + 1.85_{-\infty}$	0.048
		88−148	-6.92 ± 0.90	-15.73 ± 0.08	-2.71 ± 1.80	0.030
CaM	R106	both	-7.33 ± 0.17	-15.57 ± 0.05	-1.73 ± 0.34	0.022
		1−106	-7.34 ± 0.27	-15.58 ± 0.08	-1.72 ± 0.54	0.023
		107−148	-7.31 ± 0.26	-15.56 ± 0.08	-1.74 ± 0.51	0.022
C-domain	R106	both	-6.84 ± 0.39	-15.35 ± 0.05	-2.48 ± 0.78	0.024
		76−106	-6.78 ± 0.72	-15.33 ± 0.07	-2.59 ± 1.44	0.023
		107−148	-6.90 ± 0.49	-15.37 ± 0.07	-2.39 ± 0.98	0.021
CaM	E31[d]	32−148	-7.78 ± 0.64	-16.29 ± 0.27	$-1.55 + 1.07_{-\infty}$	0.097
CaM	R37[d]	both	-5.79 ± 3.46	-15.95 ± 0.08	$-5.19 + 2.39_{-\infty}$	0.046
		38−148	-6.20 ± 2.87	-15.92 ± 0.13	$-4.35 + 2.21_{-\infty}$	0.052

[a] Gibbs free energies fit according to eq 1 allowing heterogeneous and cooperative binding; kcal/mol (1 kcal = 4.184 J). To overestimate the uncertainty in fitted values, the greater of the positive or negative limit of each asymmetric 65% confidence interval was tabulated. [b] Estimate of cooperative free energy was calculated by eq 3, and errors were propagated by *nonlin*; this formulation provides a lower limit for the value of actual cooperativity. Both limits of asymmetric confidence intervals are shown if they differed by more than 2-fold. [c] Susceptibility curves for both peptides were analyzed simultaneously as a single data set. [d] Fits resolved from data in the phase of induced susceptibility, pCa range from 9.48 to 5.44.

ΔG_2, *span*, and $Y_{[x]_{low}}$) were allowed to float; values are reported in Table 1. Comparison of the resolved free energies (ΔG_2) for binding two calcium ions to sites III and IV indicated that the isolated C-domain had a slightly lower affinity (0.25 kcal/mol) for calcium; however, there was no difference in the calculated free energy of cooperativity (ΔG_c) for these two proteins. At least three trials for each protein were compared to confirm the magnitude and direction of this small difference.

Quantitative Proteolytic Footprinting. Quantitative proteolytic footprinting titrations of CaM using EndoGluC (*23*) and thrombin (*24*) provide residue-specific probes of calcium-induced conformational changes that may be used to estimate calcium binding energies. Calcium binding to sites I and II may be monitored by changes in the susceptibility of glutamate 31 (E31 in helix B) to cleavage by EndoGluC and arginine 37 (R37 in helix B) to cleavage by thrombin. Calcium binding to sites III and IV may be monitored by changes in the susceptibility of glutamate 87 (E87 in helix E) to cleavage by EndoGluC and arginine 106 (R106 in helix F) to cleavage by thrombin. The properties of whole CaM were compared to the isolated N-domain and C-domain.

CaM vs the Isolated C-Domain. The susceptibility profiles for both EndoGluC and thrombin footprinting of calcium binding to the isolated C-domain showed a monotonic pattern of calcium-induced protection (Figure 3). This was similar to that observed for the same residue in whole CaM with maximum cleavage occurring under apo conditions (Figure 3). From fits of the data to eq 1, the resolved free energies (ΔG_1 and ΔG_2) and the calculated free energy of cooperativity (ΔG_c) are listed in Table 1. Parameters resolved from individual analysis of complementary primary cleavage fragments (e.g., 1−87 and 88−148) are given in Table 1 to indicate the quality and consistency of data sets that contributed to the simultaneous analysis of both fragments.

Comparison of the total free energy (ΔG_2) for binding two calcium ions to CaM and the isolated C-domain indicated that the C-domain had an equivalent (0.07 kcal/mol higher) affinity as monitored by EndoGluC footprinting and a 0.22 kcal/mol lower affinity than CaM as monitored by thrombin footprinting. The calculated free energy of intradomain cooperativity (ΔG_c) was slightly higher (0.54−0.75 kcal/mol) for the isolated C-domain as monitored by both EndoGluC and thrombin.

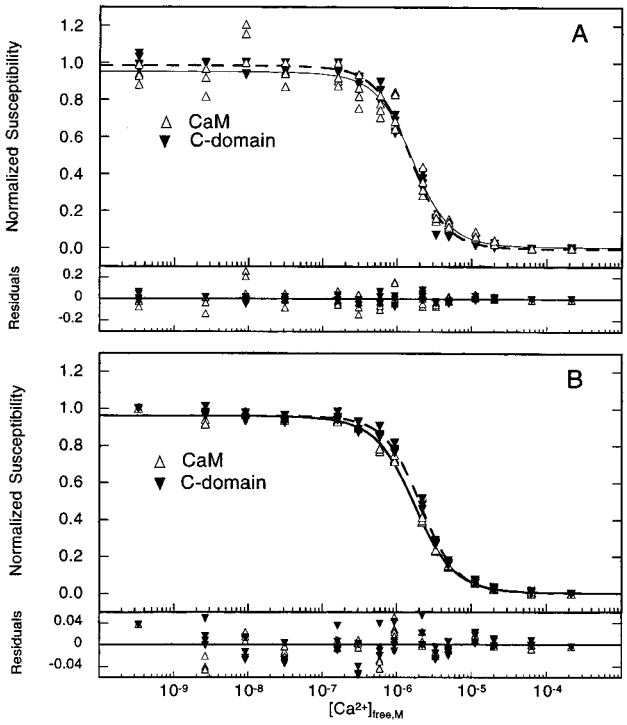

FIGURE 3: Quantitative proteolytic footprinting of the residues in the C-domain of CaM using the proteases EndoGluC (A) and thrombin (B). CaM (△) and the isolated C-domain (▼) were dialyzed in the same series of buffers (see Experimental Procedures) ranging from pCa 9.48 (apo) to 3.67 (saturating). Data presented are a composite of at least two trials. Fragments generated in thrombin proteolysis were 1−106 and 107−148 of CaM and 76−106 and 107−148 of the isolated C-domain. Fragments generated in EndoGluC proteolysis were 1−87 and 88−148 of CaM and 76−87 and 88−148 of the isolated C-domain. Curves simulated based on values given in Table 2.

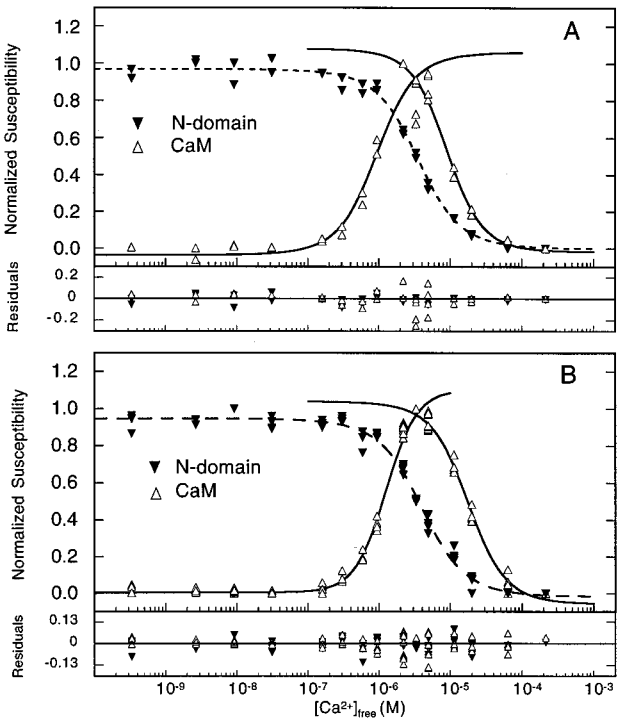

FIGURE 4: Quantitative proteolytic footprinting of the residues in the N-domain of CaM using EndoGluC (A) and thrombin (B). The isolated N-domain (▼) and CaM (△) were dialyzed in the same series of buffers (see Experimental Procedures) ranging from pCa 9.48 (apo) to 3.67 (saturating). Data shown are a composite of at least two trials. Fragments analyzed for EndoGluC proteolysis were 15−31 and 32−148 of CaM and 15−31 and 32−75 of the isolated N-domain. Fragments analyzed for thrombin proteolysis were 1−37 and 38−148 of CaM and 1−37 and 38−75 of the isolated N-domain. Curves simulated based on values given in Table 2.

CaM vs the Isolated N-Domain. Helix B of the first EF-hand in CaM (see Figure 1B) is susceptible to cleavage by EndoGluC at glutamate 31 (E31) and thrombin at arginine 37 (R37). In proteolytic footprinting titrations of whole CaM, the susceptibility profiles of these residues (Figure 4A,B) were observed to be nonmonotonic (biphasic). Unlike the calcium-induced protection of E87 and R106 in the C-domain of CaM, the susceptibility of R37 and E31 was low at both apo (pCa 9.48) and fully saturating (pCa 3.67) calcium levels. As calcium bound to sites III and IV in the C-domain (while sites I and II were vacant), the susceptibility of E31 and R37 increased sharply to a maximum (in the range of micromolar calcium). At calcium levels above micromolar (i.e., at levels sufficient for binding to sites I and II in the N-domain), conformational changes induced by local binding of calcium protected E31 and R37 from cleavage.

This alternating pattern of susceptibility indicated the presence of an intermediate conformation of the N-domain whose properties are not simply the average of the two end-states (apo and fully saturated). In sharp contrast, the susceptibility profiles of E31 and R37 in the isolated N-domain were both monotonic (Figure 4A,B), and the median calcium concentration was displaced to a lower value, indicating higher affinity. Similar to the profiles for isolated C-domain susceptibility, maximal cleavage occurred under apo conditions (pCa 9.48).

As described previously (*23*, *24*), the sharp transition observed in the biphasic susceptibility of R37 or E31 prohibited a global analysis of the complete titration. Therefore, the data were analyzed as two separate sets. The phase of induced susceptibility from pCa 9.48 to 5.44 primarily reflected properties of calcium binding to sites III and IV (see Table 2). Estimates of the energies of calcium binding to the low-affinity sites (I and II) were obtained by analyzing the phase of reduced susceptibility (i.e., increasing protection) from pCa 5.66 to 3.67 (see Table 2).

Comparison of the total free energy for binding two calcium ions (ΔG_2) to sites I and II of CaM and the isolated N-domain (Table 2) indicated that the isolated N-domain had a higher affinity for calcium, by 1.09 kcal/mol as monitored by EndoGluC and by 1.76 kcal/mol as monitored by thrombin footprinting.

Although the piecewise method of analysis can bias the precise values of free energies that were resolved from the biphasic curves, good agreement between prior studies of calcium binding to sites I and II in whole CaM using 1-D proton NMR (which provides monotonic curves based on chemical shift changes; *43*) and proteolytic footprinting (*23*, *24*) supports the differences observed here as being chemically significant. To demonstrate that the fitting approach itself could not account for the full difference between the median ligand concentrations for saturating sites I and II in the isolated N-domain vs CaM, we conducted a global analysis in which the free energies of the two phases of the CaM curves were fixed at those determined for the two isolated domains and values of both spans and intercepts were fitted. In this case, it was not possible to resolve physically meaningful fitted values of the ascending and descending spans.

This demonstrated that there is no set of parameters that can accommodate the data while keeping the domain free energies of whole CaM identical to those of the isolated domains. Thus, the observed separation in free energies is not an artifact of nonlinear least-squares analysis, and the interpretation that the isolated N-domain has a higher affinity is well-founded despite the numerical limitations in piecewise analysis. Ideally, in the future, this issue may be resolved by the availability of proteases capable of probing residues in the N-domain that have a monotonic response to calcium binding.

Gel Permeation Chromatography. Studies of the isolated domains were conducted in the absence and presence of calcium at pH 7.4 to determine the calcium-induced change in Stokes radius of the domains. Previous gel permeation chromatography studies demonstrated that the Stokes radius (R_s) of whole CaM decreased by ~1 Å (24.91 vs 23.95 Å) upon binding calcium (*44*) and these values were significantly larger than predicted based on molecular weight alone. Upon binding calcium, the R_s of both isolated domains decreased ~1 Å; the N-domain decreased from 18.16 ± 0.12 to 17.18 ± 0.00 Å, and the C-domain decreased from 18.21 ± 0.05 to 17.21 ± 0.04 Å. As expected on the basis of the large degree of sequence and structural similarity of the N- and C-domains, the domains have equivalent values of R_s at equivalent levels of calcium saturation.

Analytical Ultracentrifugation. Sedimentation equilibrium studies of CaM and the isolated N- and C-domains in the absence of calcium were conducted to determine whether the abnormal elution behavior of CaM and the isolated domains was due to self-association. Results from these studies

Table 2: Calcium Binding to Sites I and II Monitored by Quantitative Proteolytic Footprinting

protein	residue	peptide	ΔG_1[a]	ΔG_2	ΔG_c[b]	$\sqrt{\text{Var}}$
CaM	E31[c]	32−148	−6.13 ± 0.84	−13.62 ± 0.29	$-2.16 + 1.17_{-\infty}$	0.075
N-domain	E31	both[d]	−7.18 ± 0.39	−14.71 ± 0.16	−1.17 ± 0.78	0.057
		15−31	−7.15 ± 1.14	−14.67 ± 0.29	−1.18 ± 2.27	0.074
		32−75	−7.20 ± 0.33	−14.74 ± 0.14	−1.15 ± 0.67	0.036
CaM	R37[c]	both	−5.91 ± 0.55	−12.82 ± 0.13	−1.82 ± 1.11	0.055
		1−37	−5.74 ± 0.69	−12.78 ± 0.20	$-2.12 + 1.02_{-\infty}$	0.059
		38−148	−6.05 ± 0.70	−12.86 ± 0.20	−1.57 ± 1.40	0.052
N-domain	R37	both	−7.18 ± 0.21	−14.58 ± 0.11	−1.04 ± 0.45	0.038
		1−37	−7.25 ± 0.36	−14.59 ± 0.19	−0.89 ± 0.72	0.044
		38−75	−7.11 ± 0.28	−14.58 ± 0.13	−1.18 ± 0.59	0.032

[a] Gibbs free energies fit according to eq 1, allowing heterogeneous and cooperative binding; kcal/mol (1 kcal = 4.184 J). To overestimate the uncertainty in fitted values, the greater of the positive or negative limit of each asymmetric 65% confidence interval was tabulated. [b] Estimate of cooperative free energy was calculated by eq 3, and errors were propagated by *nonlin*; this formulation provides a lower limit for the value of actual cooperativity. Both limits of asymmetric confidence intervals are shown if they differed by more than 2-fold. [c] Fits resolved from data in the phase of induced protection, pCa range from 5.44 to 3.67. [d] Susceptibility curves for both peptides were analyzed simultaneously as a single data set.

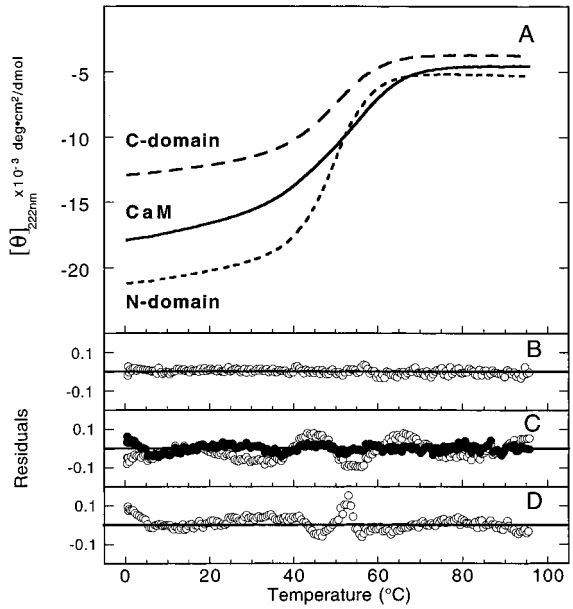

FIGURE 5: (a) Thermal unfolding studies of 15 μM C-domain (− −), CaM (—), and N-domain (− - −) per Experimental Procedures. Residuals of fits to two-state model (○, eq 4) and three-state model (●, eq 5, CaM only) based on values given in Table 3 for (B) C-domain, (C) CaM, and (D) N-domain.

indicated that calmodulin and the isolated domains are primarily monomers in solution under apo and saturating conditions at 0.5 mg/mL concentrations and the isolated N- and C-domains remain as monomers when mixed together. The average molecular mass resolved for apo CaM was 16 846 ± 1.507 g/mol (16 695 predicted from sequence); for $Ca^{2+}{}_4$-CaM, it was 15 971 ± 1.203 g/mol. Values for the isolated domains were 7647 ± 1150 g/mol for the apo N-domain (8311 predicted), 8877 ± 1013 g/mol for the $Ca^{2+}{}_2$-N-domain, 8255 ± 597 g/mol for the isolated apo C-domain (8401 predicted), and 9261 ± 595 g/mol for the $Ca^{2+}{}_2$-C-domain.

Thermal Unfolding Monitored Spectrally. Thermal unfolding of apo forms of CaM, the isolated N-domain, and the isolated C-domain was monitored by changes in circular dichroism. Figure 5A presents the molar ellipticity at 222 nm as a function of temperature. Differences in properties of the native states of these proteins and the shapes of the unfolding transitions were evident. The molar ellipticity of the native proteins (taken to be an indicator of the fraction of residues in helical conformation) was observed to be lowest for the C-domain, which was lower than whole CaM which was lower than the N-domain.

Table 3: Thermal Unfolding of Apo CaM, N-Domain, and C-Domain[a]

protein[b]	model[c]	T_m (°C)	$\Delta H°_{VH}$ (kcal/mol)	ΔC_p [cal/(K•mol)]	$\sqrt{\text{Var}}$
C-domain	N−U	49.89 ± 0.05	34.67 ± 0.18	804 ± 29	0.132
N-domain	N−U	49.73 ± 0.08	45.57 ± 0.36	727 ± 123	0.368
CaM	N−I	47.35 ± 1.15	28.14 ± 1.25		0.436
	I−U	59.95 ± 0.67	44.17 ± 1.46		
	N−U	52.41 ± 0.17	27.01 ± 0.48	604 ± 44	0.952

[a] Thermal unfolding studies were performed as described under Experimental Procedures. [b] Isolated N-domain is comprised of residues 1−75 of CaM while the C-domain consists of residues 76−148; CaM is full-length protein, residues 1−148. [c] Data were fit to two-state (N−U; eq 4) and three-state (N−I−U; eq 5) models of unfolding. In the three-state analysis of the N- and C-domain data, no best set of parameters could be selected from among multiple local minima that were found to have a strong dependence upon initial guesses.

The raw data (Figure 5A) were fit to models for two-state (eq 4; one transition) and three-state (eq 5; two transitions) unfolding processes; the resolved parameters ($\Delta H°_{VH}$, T_m, ΔC_p) are presented in Table 3. The unfolding transitions were simulated using the best-fit parameters resolved from these models. The numerical differences between the simulated transitions (for either model) and the raw data were too small to discern by visual inspection (≤0.8%); therefore, only the raw data are shown in Figure 5A; residuals are shown in Figure 5B−D.

For CaM, the residuals (Figure 5C) from a fit to the three-state model (eq 5) were much more random and had a smaller span than those from a fit to the two-state model, clearly indicating that the unfolding transition for CaM in the absence of calcium was best described by a three-state model (two unfolding transitions). The two transitions were separated by more than 10 °C in T_m and 16 kcal/mol in van't Hoff enthalpy.

The unfolding transitions for the N-domain and C-domain were fit to both the two-state and three-state models. However, the differences in the error statistics were too small to discriminate between models. Furthermore, the resolved parameters from fits of these data to the three-state model were highly dependent upon the initial guesses, indicating multiple local minima. Thus, in Table 3, for the isolated

domains, only analysis according to the two-state (single transition) model is given. Although the resolved melting temperatures of the isolated domains are almost identical, the van't Hoff enthalpy of the stability of the N-domain was approximately 11 kcal/mol more favorable than that of the C-domain. The unfolding properties of whole CaM did not correspond to a sum of these properties resolved for the two isolated domains.

DISCUSSION

Understanding the mechanism of calcium activation of CaM requires knowledge of the populated CaM conformations at intermediate levels of saturation (between zero and four calcium ions bound). These ensemble distributions are determined by the relative energies of calcium binding to each site and cooperative interactions between sites and domains. Although early studies of CaM suggested that the N- and C-domains bound calcium independently of one another (*33*, *47*), many approaches for probing energetics and conformational change in CaM have suggested otherwise. These include microcalorimetry studies (*31*, *32*, *48*), quantitative proteolytic footprinting (*23*, *24*), NMR (*27*, *43*, *49*, *50*), circular dichroism and fluorescence (*51*−*55*), and studies of site-knockout mutants of CaM (*25*, *26*).

Quantitative proteolytic footprinting titrations using the proteases EndoGluC and thrombin were used to estimate energetics of cooperative calcium binding to CaM by correlating calcium-dependent residue-specific conformational changes to site occupancy (*23*, *24*). An unexpected finding was that the proteolytic susceptibilities of bonds for residues E31, R37, and S38 in helix B in the N-domain increased in response to calcium binding to sites III and IV in the C-domain. A decrease in susceptibility was seen when calcium bound "locally" to sites I and II. This behavior was interpreted as providing direct evidence for interdomain interactions. It argued against the apo form of CaM maintaining an extended conformation similar to that observed crystallographically (Figure 1B); there, for example, the α-carbon of E31 is more than 40 Å away from the calcium ions in sites III and IV.

The biphasic susceptibility of helix B could indicate that its conformation in the apo form of whole CaM depends on the presence of the C-domain and that constraints are released upon calcium binding to sites III and IV. However, it is equally possible that there are no interactions between apo domains and that calcium binding to the C-domain initiates interactions such that helix B rearranges from a "native" state of the helix found in both whole CaM and isolated N-domain. To distinguish between these possibilities, we compared the isolated domains to CaM. Previous studies using trypsin proteolysis to generate domains resulted in a mixture of fragments terminating at lysine 75 and/or lysine 77 (*21*, *56*, *57*). Bacterial overexpression allowed the purification of homogeneous preparations of each half-molecule.

Calcium Binding to Sites III and IV. Analysis of the calcium titrations of the isolated C-domain monitored by tyrosine fluorescence (Y138, Figure 2) and quantitative proteolytic footprinting (E87 and R106, Figure 3) indicated that sites III and IV in the isolated C-domain bind calcium cooperatively as was observed for whole CaM. The resolved free energies for CaM agreed well with those reported previously (*23*, *24*); slight variations are attributed to small differences in buffer components (i.e., slightly different KCl concentrations). The difference ($\Delta\Delta G_2$) between the resolved total free energies of binding two calcium ions to sites III and IV (CaM − C-domain) ranged from −0.25 to −0.34 kcal/mol (more favorable binding to CaM; Table 1). Thus, the N-domain of whole CaM appears to have a minimal effect on the calcium binding properties of sites III and IV.

Calcium Binding to Sites I and II. The quantitative proteolytic footprinting titration of whole CaM showed a biphasic susceptibility at E31 and R37 in helix B as observed previously (*23*, *24*). In contrast, these positions in the isolated N-domain were monotonically protected by calcium binding, and their intrinsic susceptibility in the apo state was similar to the maximum value observed for whole CaM under conditions of identical proteolytic exposure. This demonstrates unequivocally that the induced susceptibility of helix B in whole CaM is caused by conformational rearrangements of the C-domain affecting the N-domain.

In agreement with previous studies (*23*, *24*, *27*, *33*, *58*−*60*), the calcium affinity of sites I and II was lower than that of sites III and IV. This was true for CaM and the isolated N-domain, but unexpectedly, there was a difference between them ($\Delta\Delta G_2$ = CaM − N-domain) of +1.1 kcal/mol (per E31) to +1.8 kcal/mol (per R37) indicating less favorable binding to CaM. Although these differences are small, they are larger than the errors of the analysis.

An advantage of the proteolytic footprinting method of monitoring an equilibrium calcium titration is that samples of each of the three proteins had been dialyzed literally in the same beaker of buffer. Thus, their calcium levels were identical, and precise conclusions regarding their relative responses can be made. Thus, we conclude that calcium binding to sites I and II is penalized by the presence of the C-domain. This difference may reflect anticooperative interactions between the domains similar to that observed in CRP dimers (*61*), or it may reflect a penalty of "assembly" (i.e., covalent linkage of the domains) analogous to the decrease in oxygen affinity that occurs when hemoglobin dimers associate to form tetramers (*62*).

This penalty is not reciprocal in magnitude for the two domains. It is interesting to note that when a pair of sites have well-separated intrinsic affinities for ligand, the free energy of cooperativity may partition such that almost all of the effect is observed as a change in the median ligand activity of the weaker site (see Figure 5 in *63*). For anticooperative interactions ($\Delta G > 0$), this will serve to separate the medians. This phenomenon may explain interactions between the "strong" C-domain and "weak" N-domain of CaM.

Biphasic Response of the N-Domain. The sharp transition in susceptibility profiles for E31 and R37 precluded simultaneous analysis of all parameters for both transitions; some subset of them had to be fixed. For this reason, the data were analyzed as two separate transitions with the numerical constraint that the maximum susceptibility of each transition is equal. This approach can introduce a bias in the resolved free energies. Although prior NMR studies of calcium titrations of whole CaM agreed well with values resolved from footprinting the same samples, we used the following approach to determine whether the $\Delta\Delta G_2$ between calcium

affinities for the N-domain and CaM could be an artifact of this fitting procedure. The biphasic profiles were fit using eq 7 [a simple sum of functions (eq 2) used in the separate analysis of the increasing and decreasing susceptibilities]:

$$F(X) = \overline{Y}_{\mathrm{I}}\mathrm{span}_{\mathrm{I}} + \overline{\overline{Y}}_{\mathrm{D}}\mathrm{span}_{\mathrm{D}} + Y_{[\mathrm{X}]_{\mathrm{low}}} \qquad (7)$$

where the subscript I refers of the phase of increasing susceptibility and D denotes the decreasing phase. Using eq 7 and fixing the values of the free energies equal to those resolved for the isolated domains, we found that the resolved values of the span were physically unreasonable (±∼7). Therefore, we conclude that estimating a nonzero value of $\Delta\Delta G_2$ is not an artifact of the fitting procedure and that the C-domain affects calcium binding to sites I and II. Studies of the isolated domains using NMR or a different protease that monitors a monotonic response for calcium binding in the N-domain will be required to hone the quantitative estimate of the difference.

Hydrodynamic Analyses. CaM was found to have a large R_s which was interpreted as reflecting its elongated shape (*44*). Calcium binding decreased the R_s of CaM. To separate the contributions of changes within domains and changes in the orientation of domains, the domains were studied individually. The R_s values of the isolated domains decreased upon calcium binding but were also notable for being much larger than predicted based on molecular weight. Although NMR solution studies of the isolated domains have demonstrated that they are not extended (*22*, *64*, *65*), the R_s values suggest that the domains are not tightly packed. Sedimentation equilibrium studies confirmed that all behaved as monomers under the conditions of this study and that the isolated domains did not interact when mixed.

Thermal Unfolding Studies. To explore whether domain interactions affected stability, apo CaM and the isolated domains were thermally denatured (Figure 5). The unfolding curves for the domains were well-described by a two-state model (single transition) with a nonzero heat capacity. Although the systematic inflections in the residuals for the fit of the N-domain (Figure 5D) suggest that the two-state model was not completely adequate, it was not possible to obtain unique fits to a three-state model for either domain. The slopes of the base lines of these curves indicate that the apo proteins at 5 °C are not tight globular units, consistent with the R_s measurements. The T_m and ΔC_p values for the isolated domains were almost identical; their enthalpies of unfolding were separated by 11 kcal/mol, consistent with calorimetric studies (*31*).

The unfolding of CaM was better described by a three-state model (two transitions) (Figure 5C; Table 3) than a two-state model (N−U). The resolved values for the two transitions were similar to other studies of CaM (*7*, *31*, *48*). However, there were notable differences when compared to the values resolved for the isolated domains. The T_m values for the transitions were no longer equivalent (ΔT_m of ∼12 °C), and the $\Delta H°_{VH}$ values were separated further ($\Delta\Delta H°_{VH}$ of ∼16 kcal/mol). Although it is simplest to assume that the two transitions correspond to the sequential unfolding of the C-domain (N−I) followed by the N-domain (I−U), it should be noted that these unfolding studies cannot provide a unique assignment of the two fitted unfolding transitions. This interpretation would be consistent with the changes in molar ellipticity seen for the isolated domains (*33*) and calorimetric comparisons (*31*).

Apo Domain Interactions. We conclude that the apo domains of CaM interact (i.e., their properties are a function of context) because the sum of the enthalpies of unfolding the isolated domains does not equal the enthalpies of each transition in whole CaM. This is in good agreement with unfolding studies of apo SynCaM and mutants (*48*). Although it is possible that the boundaries for unfolding CaM do not coincide with the division of the domains, this would still be consistent with the interpretation that the domains do not behave independently when tethered as whole CaM. The proteolytic footprinting studies also demonstrate interactions between domains. Both the energetics of calcium binding and susceptibility properties of the N-domain are linked to the presence and calcium-binding behavior of the C-domain.

An unexpected finding of this study was the 1−2 kcal/mol decrease in calcium affinity of sites I and II in CaM relative to the isolated domain. The mechanism of this difference is not understood, but the physiological consequences may be important for targets that are more sensitive to properties of one domain than the other (*8*, *66*). Evidently, both intradomain and interdomain interactions in CaM have a role in the signal transduction processes controlled by calcium activation of CaM.

ACKNOWLEDGMENT

We thank Gilson Medical Electronics for the donation of the autosampler unit for the HPLC used in this study; R. Mauer and P. Howard, University of Oregon, for the overexpression vector used for calmodulin; P. Lashmit for cloning the domains; R. E. Cohen, University of Iowa, for assistance with the sedimentation studies; J. Lary, University of Connecticut, for assistance with their numerical analysis; and the reviewers for helpful criticism.

REFERENCES

1. Kretsinger, R. H. (1976) *Annu. Rev. Biochem. 45*, 239−265.
2. Nakayama, S., and Kretsinger, R. H. (1994) *Annu. Rev. Biophys. Biomol. Struct. 23*, 473−507.
3. Klee, C. B., and Cohen, P. (1988) in *Calmodulin* (Cohen, P., and Klee, C. B., Eds.) pp 225−248, Elsevier, New York.
4. Török, K., and Whitaker, M. (1994) *BioEssays 16*(4), 221−224.
5. McPhalen, C. A., Strynadka, N. C. J., and James, M. N. G. (1991) *Adv. Protein Chem. 42*, 77−144.
6. Falke, J. J., Drake, S. K., Hazard, A. L., and Peersen, O. B. (1994) *Q. Rev. Biophys. 27*, 219−290.
7. Browne, J. P., Strom, M., Martin, S. R., and Bayley, P. M. (1997) *Biochemistry 36*, 9550−9561.
8. Kung, C., Preston, R. R., Maley, M. E., Ling, K.-Y., Kanabrocki, J. A., Seavey, B. R., and Saimi, Y. (1992) *Cell Calcium 13*, 413−425.
9. Ohya, Y., and Botstein, D. (1994) *Science 263*, 963−966.
10. Persechini, A., Stemmers, P. M., and Ohashi, I. (1996) *J. Biol. Chem. 271*, 32217−32225.
11. Haiech, J., Klee, C. B., and Demaille, J. G. (1981) *Biochemistry 20*, 3890−3897.
12. Wang, J. H., and Sharma, R. K. (1980) *Ann. N.Y. Acad. Sci. 356*, 190−204.
13. Klee, C. B. (1988) in *Calmodulin* (Cohen, P., and Klee, C. B., Eds.) pp 35−56, Elsevier, New York.
14. Bayley, P. M., and Martin, S. R. (1992) *Biochim. Biophys. Acta 1160*, 16−21.

15. Ikura, M., Spera, S., Barbato, G., Kay, L. E., Krinks, M., and Bax, A. (1991) *Biochemistry 30*, 9216−9228.
16. Persechini, A., and Kretsinger, R. H. (1988) *J. Biol. Chem. 263*, 12175−12178.
17. Small, E. W., and Anderson, S. R. (1988) *Biochemistry 27*, 419−428.
18. Pascual-Ahuir, J.-L., Mehler, E. L., and Weinstein, H. (1991) *Mol. Eng. 1*, 231−247.
19. Kretsinger, R. H. (1992) *Cell Calcium 13*, 363−376.
20. Barbato, G., Ikura, M., Kay, L. E., Pastor, R. W., and Bax, A. (1992) *Biochemistry 31*, 5269−5278.
21. Mackall, J., and Klee, C. B. (1991) *Biochemistry 30*, 7242−7247.
22. Finn, B. E., Evenäs, J., Drakenberg, T., Waltho, J. P., Thulin, E., and Forsén, S. (1995) *Nat. Struct. Biol. 2*, 777−783.
23. Pedigo, S., and Shea, M. A. (1995) *Biochemistry 34*, 1179−1196.
24. Shea, M. A., Verhoeven, A. S., and Pedigo, S. (1996) *Biochemistry 35*, 2943−2957.
25. Maune, J. F., Klee, C. B., and Beckingham, K. (1988) *J. Cell Biol. 107*, 287a (Abstract).
26. Maune, J. F., Klee, C. B., and Beckingham, K. (1992) *J. Biol. Chem. 267*, 5286−5295.
27. Starovasnik, M. A., Su, D.-A., Beckingham, K., and Klevit, R. E. (1992) *Protein Sci. 1*, 245−253.
28. Martin, S. R., Maune, J. F., Beckingham, K., and Bayley, P. M. (1992) *Eur. J. Biochem. 205*, 1107−1114.
29. Kilhoffer, M.-C., Kubina, M., Travers, F., and Haiech, J. (1992) *Biochemistry 31*, 8098−8106.
30. Giedroc, D. P., Puett, D., Sinha, S. K., and Brew, K. (1987) *Arch. Biochem. Biophys. 252*, 136−144.
31. Tsalkova, T. N., and Privalov, P. L. (1985) *J. Mol. Biol. 181*, 533−544.
32. Sellers, P., Laynez, J., Thulin, E., and Forsén, S. (1991) *Biophys. Chem. 39*, 199−204.
33. Drabikowski, W., and Brzeska, H. (1982) *J. Biol. Chem. 257*, 11584−11590.
34. Brzeska, H., Venyaminov, S. V., Grabarek, Z., and Drabikowski, W. (1983) *FEBS Lett. 153*, 169−173.
35. Drabikowski, W., Kuznicki, J., and Grabarek, Z. (1977) *Biochim. Biophys. Acta 485*, 124−133.
36. Starovasnik, M. A., Davis, T. N., and Klevit, R. E. (1993) *Biochemistry 32*, 3261−3270.
37. Sorensen, B. R., and Shea, M. A. (1997) *Biophys. J. 72*, A76 (Abstract).
38. Studier, F. W., Rosenberg, A. H., Dunn, J. J., and Dubendorff, J. W. (1990) *Methods Enzymol. 185*, 60−89.
39. Tabor, S., and Richardson, C. C. (1985) *Proc. Natl. Acad. Sci. U.S.A. 82*, 1074−1078.
40. Sorensen, B. R. (1997) Ph.D. Dissertation, University of Iowa, pp 1−312.
41. Swenson, C. A., and Fredricksen, R. S. (1992) *Biochemistry 31*, 3420−3429.
42. Johnson, M. L., and Frasier, S. G. (1985) *Methods Enzymol. 117*, 301−342.
43. Pedigo, S., and Shea, M. A. (1995) *Biochemistry 34*, 10676−10689.
44. Sorensen, B. R., and Shea, M. A. (1996) *Biophys. J. 71*, 3407−3420.
45. Eftink, M. R., Ionescu, R., Ramsay, G. D., Wong, C., Wu, J. Q., and Maki, A. H. (1996) *Biochemistry 35*, 8084−8094.
46. Carra, J. H., Anderson, E. A., and Privalov, P. L. (1994) *Biochemistry 33*, 10842−10850.
47. Cox, J. A. (1988) *Biochem. J. 249*, 621−629.
48. Protasevich, I., Ranjbar, B., Lobachov, V., Makarov, A., Gilli, R., Briand, C., Lafitte, D., and Haiech, J. (1997) *Biochemistry 36*, 2017−2024.
49. Evans, J. S., Levine, B. A., Williams, R. J. P., and Wormald, M. R. (1988) in *Calmodulin* (Cohen, P., and Klee, C. B., Eds.) pp 57−82, Elsevier, New York.
50. Seamon, K. B. (1980) *Biochemistry 19*, 207−215.
51. Klevit, R. E. (1983) *Methods Enzymol. 102*, 82−104.
52. Maune, J. F., Beckingham, K., Martin, S. R., and Bayley, P. M. (1992) *Biochemistry 31*, 7779−7786.
53. Wang, C.-L. A., Leavis, P. C., and Gergely, J. (1984) *Biochemistry 23*, 6410−6415.
54. Yao, Y., Schöneich, C., and Squier, T. C. (1994) *Biochemistry 33*, 7797−7810.
55. Anderson, S. R. (1991) *J. Biol. Chem. 266*, 11405−11408.
56. Kawasaki, H., Kurosu, Y., Isobe, T., Kasai, H., and Okuyama, T. (1986) *Anal. Sci. 2*, 287−291.
57. Walsh, M., Stevens, F. C., Kuznicki, J., and Drabikowski, W. (1977) *J. Biol. Chem. 252*, 7440−7443.
58. Wang, C.-L. A. (1985) *Biochem. Biophys. Res. Commun. 130(1)*, 426−430.
59. Crouch, T. H., and Klee, C. B. (1980) *Biochemistry 19*, 3692−3698.
60. Klee, C. B. (1977) *Biochemistry 16*, 1017−1024.
61. Heyduk, T., and Lee, J. C. (1989) *Biochemistry 28*, 6914−6924.
62. Holt, J. M., and Ackers, G. K. (1995) *FASEB J. 9*, 210−218.
63. Ackers, G. K., Shea, M. A., and Smith, F. R. (1983) *J. Mol. Biol. 170*, 223−242.
64. Kuboniwa, H., Tjandra, N., Grzesiek, S., Ren, H., Klee, C. B., and Bax, A. (1995) *Nature Struct. Biol. 2*, 768−776.
65. Zhang, M., Tanaka, T., and Ikura, M. (1995) *Nature Struct. Biol. 2*, 758−767.
66. George, S. E., VanBerkum, M. F. A., Ono, T., Cook, R., Hanley, R. M., Putkey, J. A., and Means, A. R. (1990) *J. Biol. Chem. 265(16)*, 9228−9235.
67. Kraulis, P. J. (1991) *J. Appl. Crystallogr. 24*, 946−950.
68. Babu, Y. S., Bugg, C. E., and Cook, W. J. (1988) *J. Mol. Biol. 204*, 191−204.
69. Bernstein, F. C., Koetzle, T. F., Williams, G. J. B., Meyer Jr., E. F., Brice, M. D., Rodgers, J. R., Kennard, O., Shimanouchi, T., and Tasumi, M. (1977) *J. Mol. Biol. 112*, 535−542.
70. Abola, E. E., Bernstein, F. C., Bryant, S. H., Koetzle, T. F., and Weng, J. (1987) in *Crystallographic Databases—Information Content, Software Systems, Scientific Applications* (Allen, F. H., Bergerhoff, G., and Sievers, R., Eds.) pp 107−132, Data Commission of the International Union of Crystallography, Bonn/Cambridge/Chester.

BI9718200